

Microstructured poly(N-isopropylacrylamide) hydrogels with fast temperature response for pulsatile drug delivery

K. Palomino¹ · K. A. Suarez-Meraz¹ · A. Serrano-Medina¹ · A. Olivas² · E. C. Samano² · J. M. Cornejo-Bravo¹

Received: 21 May 2015 / Accepted: 11 September 2015 / Published online: 24 September 2015
© Springer Science+Business Media Dordrecht 2015

Abstract Microstructured, temperature-sensitive poly(N-isopropylacrylamide) hydrogels were prepared with different proportions of poly(N-isopropylacrylamide) microparticles. The materials presented fast shrinkage at a temperature above their transition temperature (LCST = 32 °C), with highly reproducible swelling/shrinking cycles when temperature oscillates between below and above the LCST. They showed positive solute release control as a function of the temperature when small amount of microparticles were included in the hydrogels, making these hydrogels suitable for temperature controlled pulsatile drug release. The degree of crosslinking had a smaller impact than the percentage of microparticles in swelling and drug release in response to temperature. The inclusion of a small proportion of microparticles improved the mechanical properties of the hydrogels. In addition, the polymerization steps are carried on in aqueous media, being a facile, scalable, and environmentally friendly technology.

Keywords Hydrogels · p-NIPAAm · Drug delivery · Microparticles

Introduction

Materials that respond to external stimuli are called “smart materials”. Hydrogels belong to these types of materials because their degree of swelling, for instance, can be modified in response to external stimuli such as temperature, pH, ionic strength, and voltage [1].

One of most studied thermoresponsive materials is Poly(N-isopropylacrylamide) (PNIPAAm) that exhibits a temperature induced volume phase transition, from a swollen phase to a contracted phase, at a low critical solution temperature (LCST) of 32 °C [2, 3]. Because of this property, PNIPAAm hydrogels have applications in drug delivery [4–6], separation processes [7], and thermoresponsive gates [8], among others.

In particular, protein and peptide therapeutics produce better pharmacodynamic responses when administrated in pulses to avoid down regulation control [9–14]. In this paper, we propose the use of pulsatile drug delivery based on environmentally sensitive hydrogels since swelling controlled release can be modulated to respond to changes in the environment (e.g., temperature, pH) produced by diseases, circadian cycles, or externally induced factors [15–17]. However, hydrogels suffer from certain limitations such as slow response rates [18] and poor mechanical properties [19]. In particular, PNIPAAm hydrogels undergo vitrification during the shrinking process above the LCST. A dense “skin” layer on the surface of these hydrogels is formed that it inhibits water loss from within [20].

Most strategies to produce fast responding hydrogels are based on the production of micropores in the hydrogels through which water and solutes are expelled during hydrogel shrinkage [20–28]. Microporous structures are spongy and have low mechanical strength, thus solute release is not very reliable due to possible rupture of the hydrogel matrix during application [26].

✉ J. M. Cornejo-Bravo
jmcornejo@uabc.edu.mx

¹ Universidad Autónoma de Baja California, Calzada Universidad 14418 Parque Industrial Internacional, Tijuana, Baja California 22300, Mexico

² Centro de Nanociencias y Nanotecnología, Universidad Nacional Autónoma de México, Km. 107 Carretera Tijuana-Ensenada C.P., 22860 Ensenada, B.C., Mexico

In this work, we prepared hydrogels of PNIPAAm with different proportions of PNIPAAm microparticles (MP) having a hydrodynamic diameter of 585 nm. Even though these hydrogels are not microporous, they show fast shrinking. We suggest that the fast shrinkage occurs because micropores are produced due to fast contraction of the microgels when the temperature rises above LCST. This fast mechanism allows water ejection during (macro)hydrogel shrinkage, and reversible swelling/shrinking when temperature oscillates between 25 and 40 °C. The mechanical properties of the hydrogels are also improved showing an increase in the reduced elastic modulus as the percentage of microparticles inclusion rises. These properties make these materials suitable for temperature controlled pulsatile drug delivery. Regarding this issue, the release of vitamin B₁₂ and cytochrome C loaded into the microstructured hydrogels are investigated in the LCST range.

Experimental

Materials

NIPAAm (TCI, 98 %) was recrystallized from n-hexane. N, N-methylenebisacrylamide (BIS) (Aldrich, 98 %), ammonium persulfate (APS) (Aldrich, 98 %), N, N, N, N tetramethylethylenediamine (TEMED) (Aldrich, 99.5 %), cytochrome C (Sigma-Aldrich), and vitamin B₁₂ (Sigma Aldrich) were used as received. Ethyleneglycoldimethylacrylate (EGDMA) (Aldrich, 98 %) was purified by passing the monomer through an inhibitor remover resin (Aldrich). Distilled water was put through a filter with a 0.22 μm pore size to eliminate any particulate matter before using it.

Synthesis of microparticles

MPs were prepared by dispersion polymerization [29, 30]: 0.5 g of NIPAAm and 0.043 g of EGDMA were added to 50.0 mL of distilled water. The solution was stirred for 30 min while being purged in argon to remove oxygen. The solution was heated to 85 °C in an oil bath for 30 min, and then 0.04 g of APS dissolved in 0.8 mL of distilled water was added to start the reaction. Stirring was maintained at 300 rpm. The reaction was run for 45 min and stopped by placing the reaction vessel in water/ice bath. The resulting dispersions were purified for 5 days by dialysis using a regenerated cellulose membrane with a 14 kDa molecular weight cutoff (Spectrum Laboratories). MPs were recovered by freeze drying.

Microparticles characterization

The purified (dialyzed and freeze-dried) MPs were redispersed in distilled water (1.0 mg/mL). The hydrodynamic diameter (D_h) was measured by dynamic light scattering

(DLS) using a Zetasizer Nano NS (DTS 1060; Malvern Instruments, Miami, FL, USA) equipped with a green laser of 532 nm. The angle of measurement was 173° (backscattering). The size distribution reported is the distribution by intensity. The effect of the temperature on the particle size of the MP was studied by DLS using the same Zetasizer Nano equipment by a temperature trend method from 20 to 50 °C every 2 °C.

Synthesis of PNIPAAm hydrogels

In the second stage of the polymerization, hydrogels were prepared with different weight ratios of NIPAAm to MP (NIPAAm/MP 100/0, 92.5/7.5, 85/15, and 70/30), crosslinked by BIS at 4.5 w%. The recipe used was as follows: 1.58 g of NIPAAm + MPs were dispersed in 7.92 g of distilled water, followed by 0.072 g BIS, and stirred for 15 min. Then, 1.03 mL of APS 0.15 M and 1.03 mL of TEMED 0.15 M were added to the mixture. The solution was placed between two glass plates, previously silanized. The polymerization of hydrogels was carried out at 4 °C for 24 h. A hydrogel was prepared with double proportion of cross-linked (9 w%) (NIPAAm/MP 85/15 DC). Finally, the hydrogels were cut into discs of 1 cm in diameter with a lab puncher. The hydrogels were washed with distilled water at room temperature for 5 days.

Characterization of hydrogels

Scanning electron microscopy of hydrogels

The structure and morphology of the samples were studied by a scanning electron microscope (Hitachi-X650). Hydrogels were swollen to equilibrium at 25 °C, frozen in liquid nitrogen, and freeze-dried afterwards. Next, the hydrogel samples were broken and coated with gold for visualization by an electron beam.

Determination of equilibrium swelling ratio

The equilibrium swelling degree, Q, was determined as function of temperature. Q is given by:

$$Q = (W_s - W_d) / W_d \quad (1)$$

where W_s is the weight of a hydrogel swollen to equilibrium at a given temperature, and W_d is that of the dry gel. The W_s values were obtained by weighing a hydrogel after blotting the excess of superficial water with filter paper at the 20 to 40 °C temperature range and recorded until samples reached constant weight. The LCST is determined as the maximum change in weight with temperature.

Swelling kinetics study

The kinetics of swelling of the hydrogels was measured gravimetrically at 25 °C (below the LCST) recording the weight during swelling at different times. Q_t is given by:

$$Q_t = (W_t - W_d) / W_d \quad (2)$$

where W_t is the weight at the sampling time, and W_d is defined as before.

Shrinking kinetics

The shrinking kinetics of the hydrogels was measured gravimetrically at 40 °C (above the LCST). Before the shrinking measurements, the gels were swollen to equilibrium weight in distilled water at 25 °C. Then they were immersed into distilled water at 40 °C, recording the weight during collapsing at different times. Water retention is defined as follows:

$$\text{Water Retention} = 100 \times (W_t - W_d) / W_s \quad (3)$$

where W_t is the weight of the hydrogel at the sampling time, the other symbols are the same as above.

Oscillating shrinking-swelling kinetics

The hydrogel discs were swollen to equilibrium in distilled water at 25 °C, and then the temperature was cycled between 40 and 25 °C every hour with constant agitation. The hydrogels were weighted every 15 min.

Mechanical properties of the hydrogels

The mechanical properties of the hydrogel discs were measured using a TriboScope nanoindenter, Hysitron. The nanoindenter is used in conjunction with an atomic force microscope (AFM) so that the sampling area can be visualized with the same probe before and after every indentation. The probe is a commercial Berkovich diamond tip attached to a transducer. This unit replaces the conventional optical head with a cantilever of a commercial AFM. The tip penetrates into the sample from zero up to a maximum predetermined force (loading region); then the tip returns to its original position (unloading region). The Young's modulus of the samples was found from the unloading region of the indentation curve using the Oliver and Pharr theory [31].

Loaded and release of model substances into hydrogels

Model substances were loaded by swelling the hydrogels in a phosphate buffer, pH 7.4, containing 10 mg/mL vitamin B₁₂ or cytochrome C at 4 °C for 7 days. Before the release experiments, the loading solutions containing the hydrogels were

equilibrated at 25 °C. Afterwards, the loaded hydrogels were placed in 3 mL buffer solution, pH 7.4, at 25 °C, maintaining moderated agitation by means of a magnetic stirrer. Samples (1 mL) were withdrawn every 15 min, and replaced with fresh buffer solution. After 1 h, the hydrogels were placed in 3 mL buffer, pH 7.4, at 40 °C for 1 h and the same sampling protocol as before was followed. Then, the samples were placed in media at 25 °C, with the same sampling procedure. The temperature cycles were repeated until complete solute release was obtained. Release of vitamin B₁₂ and cytochrome C was followed by UV–Vis spectroscopy at 361 and 528 nm, respectively. Solute loading was calculated from the amount of drug released after complete release was observed.

Results and discussion

MP synthesis and characterization

Monodispersed MPs were obtained with an average diameter (D_h) of 585 nm at 25 °C (PDI=0.136). The size distribution of the microparticles and the effect of temperature on their size are shown in Fig. 1a and b, respectively. The LCST is defined as the maximum size change and occurs at 32 °C, with a size of 285 nm above the LCST. EDGMA was selected as the crosslinker for the synthesis of MPs due to the good swelling/deswelling properties produced with this crosslinker, found in a previous study [30].

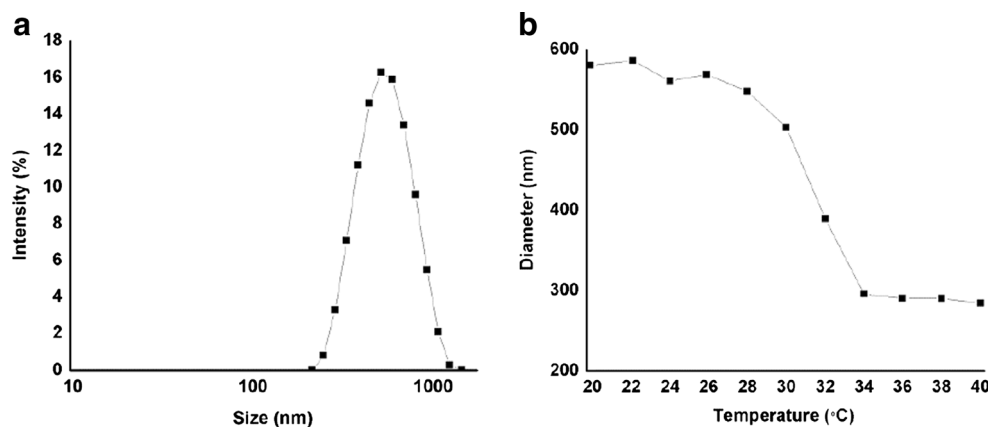
Hydrogels preparation

MPs are swollen with the polymerization mixture, as described in “[Synthesis of microparticles](#)”, during hydrogel formation, thus the hydrogel chains are formed, and chain entanglement is produced [32–34]. The swollen *NIPAAm/MP* 100/0 hydrogel is transparent, soft, and fragile. However, the samples with microstructured hydrogels are opaque; the degree of opacity increases as the proportions of MPs is increased, indicating that MP introduce inhomogeneities during hydrogel synthesis. The surface morphology of the hydrogels was investigated by SEM and micrographs are displayed in Fig. 2. The surface of the *PNIPAAm/MP* 100/0 samples are homogeneous and smooth, as shown in Fig. 2a. Although the morphology changes as the content of the microstructured hydrogels is increased in the samples, the surface tends to be irregular and rough, as shown in Fig. 2b, and even spongy, as shown in Fig. 2c.

Effect of temperature on equilibrium swelling ratio

Figure 3 shows the swelling degree Q for all hydrogels, as a function of temperature in the 20 to 40 °C range. They all have the greatest value of Q at 20 °C, which continuously decreases

Fig. 1 **a** Size distribution of the PNIPAAm microparticles at 25 °C, and **b** change of microparticle size as a function of temperature



with increasing temperature until $T \approx 34$ °C where an abrupt change occurs. The value of Q remains basically constant when $T \geq 34$ °C. The *NIPAAm/MP 100/0* and *92.5/7.5* hydrogels have similar degree of swelling at 20 °C, *NIPAAm/MP 85/15* has slightly higher degree of swelling, and *NIPAAm/MP 70/30* has 20 % higher degree of swelling, which is attributed to the inhomogeneities introduced for the MP. The hydrogel *NIPAAm/MP 85/15 DC* shows the lowest Q , as expected due to higher crosslink density and, for instance, a higher elastic force against swelling.

These results differ from those obtained by Fernandez et al. for nanostructured *PNIPAAm* hydrogels [32]. In the first state of polymerization, they prepared nanogels with an average diameter of 29.5 nm by an inverse emulsion polymerization technique and observed a higher equilibrium swelling as the proportion of nanogels increases. They observed that values of Q for the nanostructured hydrogels are up to six times greater than the conventional *PNIPAAm* hydrogel. They argue that the nanogels have a higher mass density than the macro-hydrogels and this introduces inhomogeneities in the material during the second state of polymerization (macrohydrogel formation), and porous materials are produced. As the proportion of nanoparticles increases, there is an increase on the porosity and, as a consequence, water uptake [32, 34].

In our study we use MP produced by a dispersion polymerization method with a volume about 400 times the volume used in the published study. The swelling ratio of the microparticles, defined as $[(D_{h, 25^\circ C}/D_{h, 40^\circ C})^3]$, is 8.64 which is similar to the degree of swelling of the microstructured hydrogels. This indicates that microparticles and hydrogels have similar mass densities, for instance, MP does not produce porosity in a high extent. Only the hydrogel with the maximum proportion of MP studied (30 w%) presents a slightly higher swelling at equilibrium compared to the rest of the hydrogels. Besides, in our case, the degree of swelling of the microstructured hydrogels (below the LCST) is about one order of magnitude smaller than the reported with highly porous

systems [26, 27, 35, 36], which is also indicative of distinct microstructure characteristics.

Swelling kinetics

Figure 4 shows the swelling kinetics starting from dry hydrogels at 25 °C. All curves in this figure are similar, meaning that the hydrogels have a comparable swelling kinetics because crosslinking density and porosity are alike. As shown in the inset in Fig. 4, the swelling rate decreases as a function of the elapsed time for all hydrogels [32]. At the beginning of the process, the *NIPAAm/MP 85/15 DC* hydrogel has the slowest swelling kinetics due to its higher crosslinking density. The initial rate of swelling increases with the proportion of MP, which can be attributed to the heterogeneity introduced by MP; however, the hydrogel *NIPAAm/MP 100/0* presents initial swelling rate similar to the *NIPAAm/MP 70/30*. Since MPs act as crosslinker points, *NIPAAm/MP 100/0* hydrogels has the lowest overall crosslinking density of all the hydrogels studied and that may explain the high initial swelling rate observed.

Shrinking kinetics is shown in Fig. 5 for all samples in the 25 to 40 °C temperature range. Conventional *PNIPAAm* hydrogels present very low shrinking kinetics due to the formation of a stiff layer skin-like on the surface of the hydrogel that blocks water diffusion [19, 20]. The inclusion of 7.5 w% of MP produces only a slight increase in shrinking kinetics. On the other hand, hydrogels containing MP at 15 w% (with both crosslink proportions), and 30 w% present very fast shrinking kinetics almost reaching the minimum of water retention (8 %) at the first sampling time (2 min), except for the hydrogel with double crosslinking proportion was lowest with 19 % water retention.

The results are similar to those obtained by highly porous *PNIPAAm* hydrogels where fast shrinking occurs by water ejection through the pores of the hydrogels [19, 36].

However, porosity itself does not explain the results for hydrogels studied in this work. As mentioned previously, the

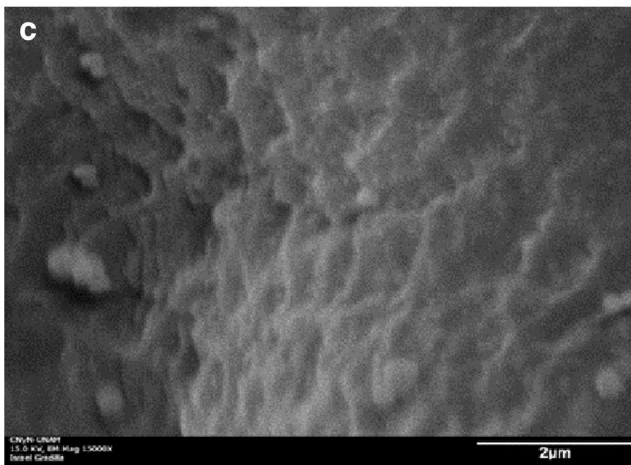
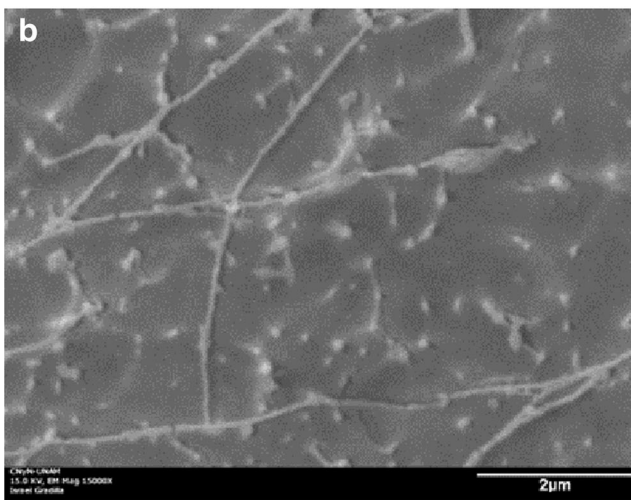
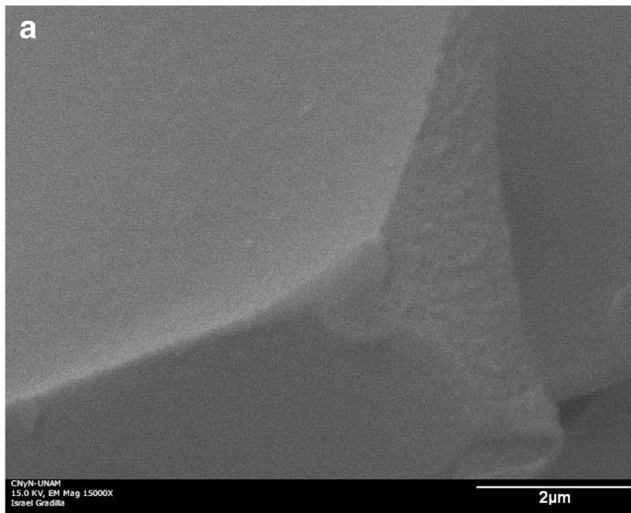


Fig. 2 SEM micrographs of hydrogels: **a** *NIPAAm/MP* 100/0, **b** *NIPAAm/MP* 85/15, **c** *NIPAAm/MP* 70/30

equilibrium swelling below the LCST is one order of magnitude smaller than that for porous PNIPAAm hydrogels. Besides, the hydrogels *NIPAAm/MP* 85/15 % and *NIPAAm/MP*

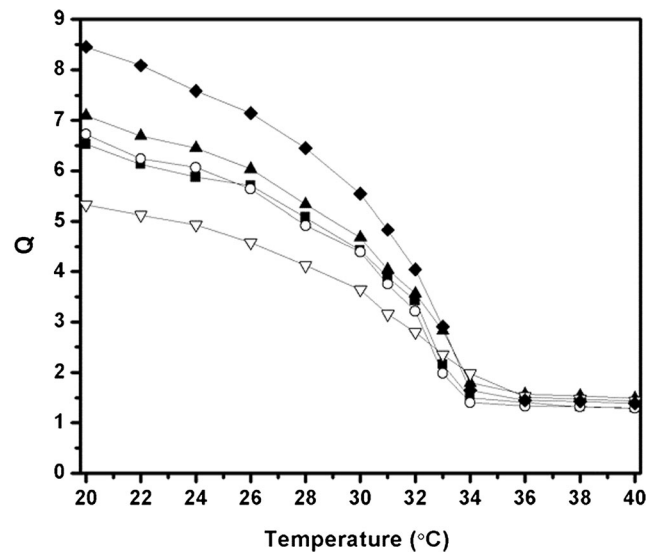


Fig. 3 Temperature dependence of equilibrium swelling degree of PNIPAAm hydrogels: (■) *NIPAAm/MP* 100/0, (O) *NIPAAm/MP* 92.5/7.5, (▲) *NIPAAm/MP* 85/15, (▽) *NIPAAm/MP* 85/15 DC, (◆) *NIPAAm/MP* 70/30

92.5/7.5 % have about the same degree of swelling at equilibrium, but different shrinking kinetics. For instance, we hypothesize that the fast shrinking kinetics for the microstructured hydrogels are due to a fast contraction of microparticles creating micropores that allow water diffusion during macro-hydrogel contraction (see Fig. 6). We base our hypothesis on two facts: first, microgels included in hydrogels maintain their swelling/shrinking properties [37]; and second, the rate of response of microgels is considerable faster than the macro-hydrogels, since rate of response is inversely

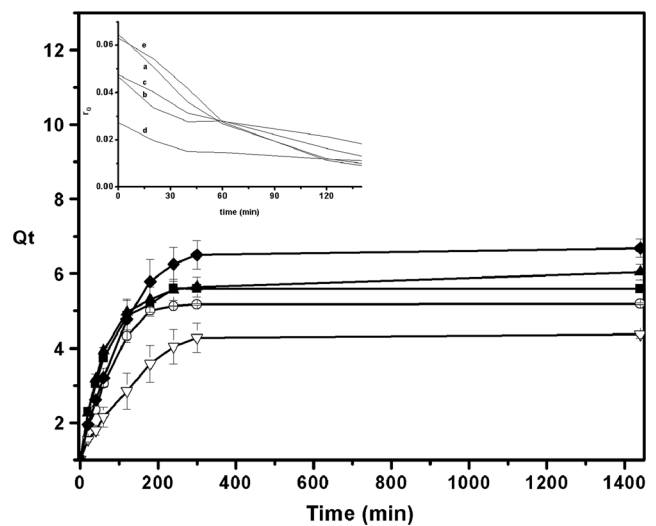


Fig. 4 Degree of swelling as a function of time at 25 °C for hydrogels: (■) *NIPAAm/MP* 100/0, (O) *NIPAAm/MP* 92.5/7.5, (▲) *NIPAAm/MP* 85/15, (▽) *NIPAAm/MP* 85/15 DC, (◆) *NIPAAm/MP* 70/30. Inset: Swelling rate ($\Delta Q/\Delta t$) as a function of time: **a** *NIPAAm/MP* 100/0, **b** *NIPAAm/MP* 92.5/7.5, **c** *NIPAAm/MP* 85/15, **d** *NIPAAm/MP* 85/15 DC, **e** *NIPAAm/MP* 70/30

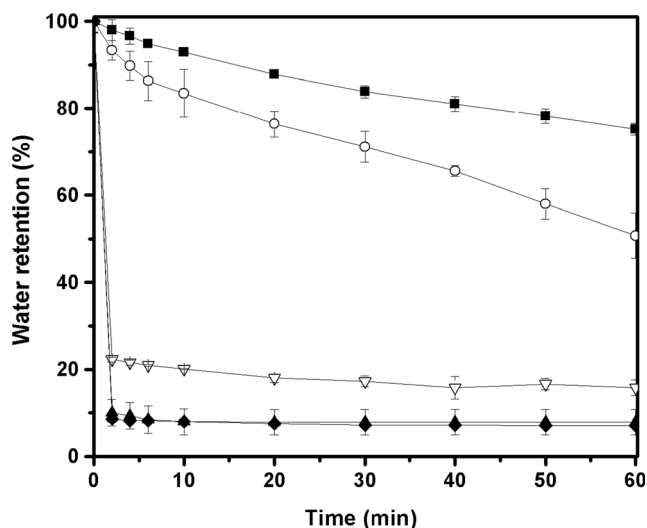


Fig. 5 Shrinkage kinetics for hydrogels: (■) *NIPAAm/MP* 100/0, (○) *NIPAAm/MP* 92.5/7.5, (▲) *NIPAAm/MP* 85/15, (▼) *NIPAAm/MP* 85/15 DC, (◆) *NIPAAm/MP* 70/30. (*NIPAAm/MP* 85/15, and *NIPAAm/MP* 70/30 (data are superimposed))

proportional to the square of the smallest spatial dimension of the hydrogel [18].

The inclusion of a very small proportion of MP in the hydrogels (e.g., 7.5 w%) is not enough to form pores that percolate the hydrogels and allows complete water expulsion when the hydrogel shrinks at temperature above the LCST.

Shrinking and swelling cycles at 40 and 25 °C, respectively, with a sampling time of 60 min per cycle are used to determine the relative swelling degree for all samples, as observed in Fig. 7 for three shrinking/swelling cycles. The curve for the *NIPAAm/MP* 100/0 hydrogels shows a small variation on the relative swelling degree in each cycle due to the formation of the skin layer at 40 °C, which results in a negligible temperature response for this hydrogel. The slope on the curve for the shrinking cycle of the *NIPAAm/MP* 92.5/7.5 hydrogel is steeper than the slope for the swelling one. Therefore, there

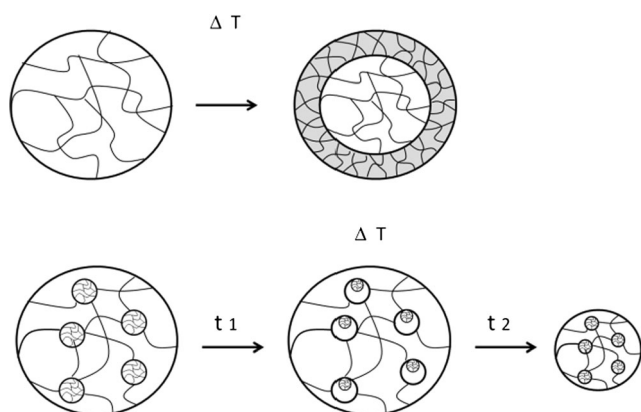


Fig. 6 Proposed mechanism for the shrinking process in thermosensitive hydrogels. Formation of a skin-like layer in a conventional PNIPAAm hydrogel (top). Formation of micropores by the contraction of the microgels followed by shrinkage of the macro-hydrogel (bottom)

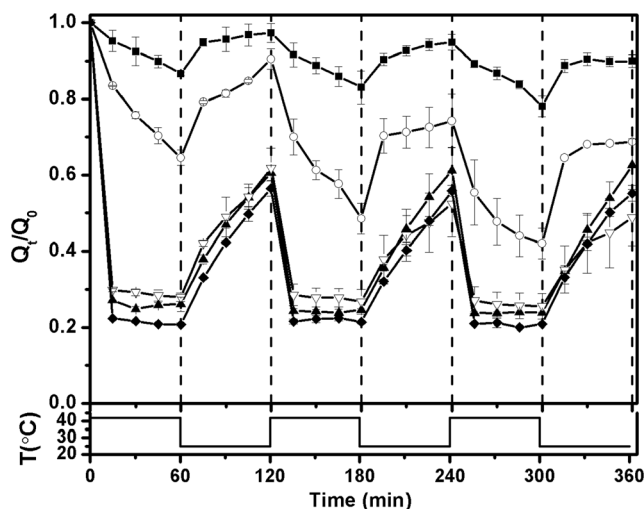


Fig. 7 Relative swelling degree (Q_{t40}/Q_{25}) with cycles of temperature between 25 and 40 °C: (■) *NIPAAm/MP* 100/0, (○) *NIPAAm/MP* 92.5/7.5, (▲) *NIPAAm/MP* 85/15, (▼) *NIPAAm/MP* 85/15 DC, (◆) *NIPAAm/MP* 70/30

is a decrease of the peaks height (local maxima) for the relative swelling degree after one full cycle (one shrinking + one swelling). For instance, the Q_t/Q_0 value drops from 1 to 0.9 after the first full cycle and then to 0.68 at the end of the third cycle, as shown in Fig. 7. The other curves for the relative swelling degree for the remaining samples show an oscillating behavior very similar in between, so that the reproducible swelling/shrinking curves are produced in each temperature oscillation.

The average Young's modulus values measured by nanoindentation are shown in Table 1. There is an increase in the Young modulus of 40 % after adding just 7.5 % of MPs. An increase in the Young modulus has been observed with nanostructured hydrogels because the nanoparticles act as a crosslinking points [32–34]. The hydrogel *NIPAAm/MP* 70/30 has an average Young modulus only slightly higher than the conventional *PNIPAAm* hydrogel. This is probably due to the porosity of this hydrogel.

Macromolecules loading and release

Table 1 presents drug loadings of the hydrogels as well. Similar loadings are observed for all hydrogels except for the hydrogel *NIPAAm/MP* 85/15 DC due to its lower swelling capacity.

Release of vitamin B₁₂ (1335 Da) with temperature cycles between 25 and 40 °C is shown in Fig. 8a. Considerable release is observed in the first hour at 25 °C for all hydrogels except the hydrogel *NIPAAm/MP* 92.5/7.5. Temperature jump to 40 °C halts drug release for the *NIPAAm/MP* 100/0 hydrogel. Decreasing the temperature to 25 °C reinitiates drug release. These results confirm the formation of a dense skin on the surface of the hydrogel that blocks drug release when

Table 1 Mechanical properties and solute loading of the hydrogels studied

Hydrogel <i>NIPAAm/MP</i> %w	Young's modulus (GPa)	Loading vitamin B ₁₂ (mg/g)	Loading cytochrome C (mg/g)
100/0	2.02	0.604	0.527
92.5/7.5	2.79	0.555	0.556
85/15	2.61	0.587	0.577
85/15 DC	2.48	0.332	0.303
70/30	2.13	0.502	0.477

temperature is raised above the LCST. For hydrogel *NIPAAm/MP* 70/30 release is extensive at 25 °C in the first hour (>80 %), and no effect of increasing the temperature is observed. These results are attributed to the higher swelling of this hydrogel. For the hydrogels *NIPAAm/MP* 85/15, with

both degrees of crosslinker, the release is also extensive at 25 °C, but an increase on rate of release is observed at temperature above the LCST (Fig. 8b). In these cases all drug is released in the first cycle of temperature. The hydrogel

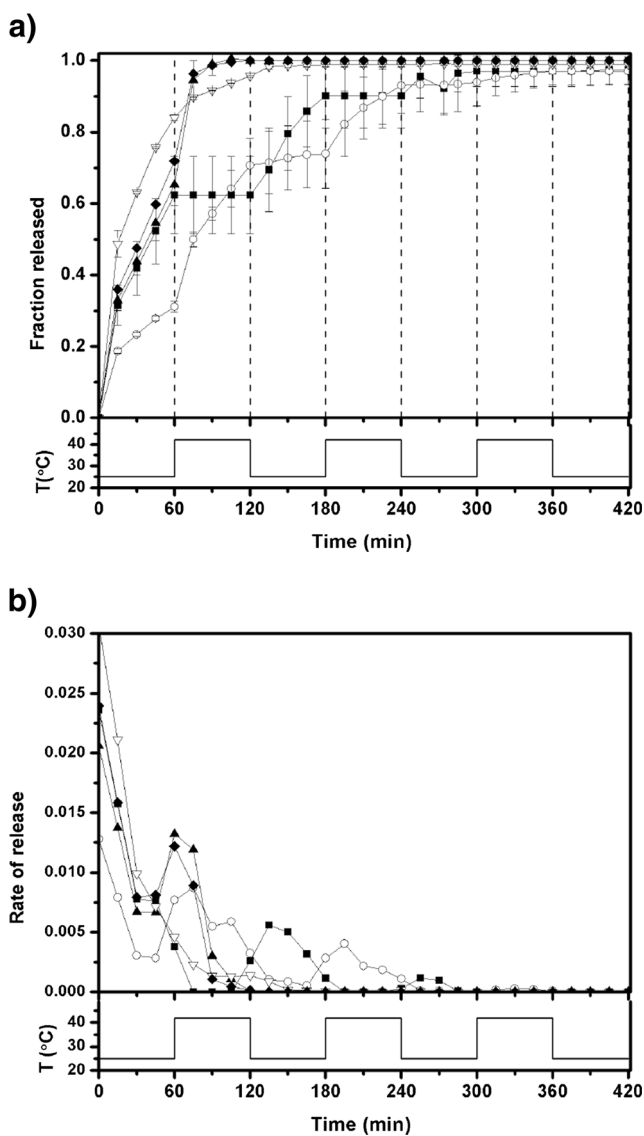


Fig. 8 a Releasing vitamin B₁₂ in cycles of temperature and b rate of release (mg/min) normalized by the drug loading: (■) *NIPAAm/MP* 100/0, (○) *NIPAAm/MP* 92.5/7.5, (▲) *NIPAAm/MP* 85/15, (◆) *NIPAAm/MP* 85/15 DC, (▽) *NIPAAm/MP* 70/30

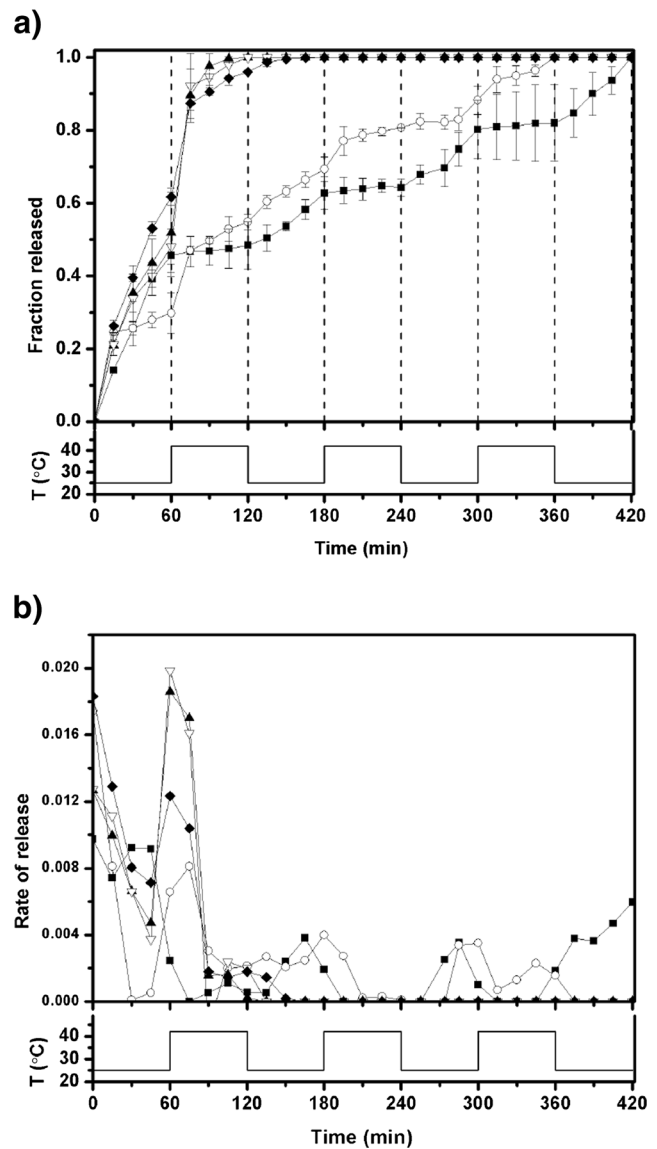


Fig. 9 a Releasing of cytochrome C in cycles of temperature and b rate of release (mg/min) normalized by the drug loading: (■) *NIPAAm/MP* 100/0, (○) *NIPAAm/MP* 92.5/7.5, (▲) *NIPAAm/MP* 85/15, (◆) *NIPAAm/MP* 85/15 DC, (▽) *NIPAAm/MP* 70/30

NIPAAm/MP 92.5/7.5 shows a smaller release in the first hour at 25 °C and a clear increase in rate of release at 40 °C, decreasing the rate of release as the temperature is back at 25 °C. The process is repeated in each cycle of temperature but the amount of drug released decreases in each temperature cycle as the release becomes complete.

Figure 9a presents cytochrome C (12,000 Da) release with cycles of temperature. Rate of release is somewhat slower than for vitamin B₁₂ due to the higher molecular weight of cytochrome C. For the hydrogel *NIPAAm/MP 100/0* drug release is halted at 40 °C in each cycle and release only occurs at 25 °C, as observed for vitamin B₁₂. For the hydrogels *NIPAAm/MP 85/15* (both crosslinker proportions) and *NIPAAm/MP 70/30* a clear increase on rate is observed at 40 °C (Fig. 9b) with the whole load released in the first temperature cycle. For the hydrogel *NIPAAm/MP 92.5/7.5* pulses of release are observed at 40 °C in each cycle, taking three cycles for complete release of the solute.

Conclusion

Inclusion of PNIPAAm microparticles in PNIPAAm hydrogels produces fast thermoresponsive materials with improved mechanical properties. The microstructured hydrogels present similar swelling at equilibrium than the conventional PNIPAAm hydrogels indicating similar porosities. We propose that fast shrinking of microstructured hydrogels above the LCST is due to the formation of micropores by the contraction of the MP before macro-hydrogel shrinkage, allowing water expulsion and avoiding the formation of a skin-like layer on the surface of the hydrogels. Conventional PNIPAAm hydrogels present a skin-like formation and shows negative solute control on drug release (release below the LCST). On the other hand, microstructured hydrogels present positive drug release control. Pulsatile solute release controlled by temperature can be obtained when small proportion of MP are included in the hydrogels, otherwise release is too fast for a controlled release system. The degree of crosslinking has a smaller impact than the proportion of MP in swelling and drug release in response to temperature.

Fast release of solutes was obtained when temperature raise above the LCST, indicating that these systems can be used to release therapeutic agents that require peaks in the serum concentration at predetermined intervals (e.g., hormones) [38].

A facile and scalable method was adapted to produce materials with fast temperature response and improved mechanical properties with high potential for application in several fields, including drug delivery. All the polymerization steps are carried on in aqueous media, being an environmentally friendly technology.

Acknowledgments Work supported by SEP-CONACYT grant (CB2010-1-157173) and (C0010-2011-01- 174492). JM CB thanks CONACYT for Abroad Sabbatical Stay fellowship (232833).

References

- Bhattacharya S, Eckert F, Boyko V, Pich A (2007) Temperature-, pH-, and magnetic-field-sensitive hybrid microgels. *Small* 3(4): 650–657
- Taylor L, Cerankowski L (1975) Preparation of films exhibiting a balanced temperature dependence to permeation by aqueous solutions—a study of lower consolute behavior. *J Polym Sci Polym Chem* 13(11):2419–2639
- Hirokawa Y, Tanaka T (1984) Volume phase transition in a nonionic gel. *J Chem Phys* 81(12):6379–6380
- Gutowska A, Bae YH, Jacobs H, Mohammed F, Mix D, Feijen J, Kim SW (1995) Heparin release from thermosensitive polymer coatings: in vivo studies. *J Biomed Mater Res* 29(7):811–821
- Vakkalanka S, Brazel C, Peppas N (1997) Temperature- and pH-sensitive terpolymers for modulated delivery of streptokinase. *J Biomater Sci Polym* 8(2):119–129
- Chung JE, Yokoyama M, Yamato M, Aoyagi T, Sukurai Y, Okano T (1999) Thermo-responsive drug delivery from polymeric micelles constructed using block copolymers of poly(N-isopropylacrylamide) and poly(butylmethacrylate). *J Control Release* 62(1-2):115–127
- Freitas RF, Cussler EL (1987) Temperature sensitive gels as extraction solvents. *Chem Eng Sci* 42(1):97–103
- Chu LY, Park SH, Yamaguchi T, Nakao S (2001) Preparation of thermo-responsive core-shell microcapsules with a porous membrane and poly(N-isopropylacrylamide) gates. *J Membr Sci* 192(1-2):27–39
- Hulse JA, Rosenthal SM, Cutler L (1986) The effect of pulsatile administration, continuous infusion, and diurnal variation on the growth hormone (GH) response to GH-releasing hormone in normal men. *J Clin Endocrinol Metab* 63(4):872–878
- Tam CS, Heersche JN, Murray TM (1982) Parathyroid hormone stimulates the bone apposition rate independently of its resorptive action: differential effects of intermittent and continuous administration. *Endocrinology* 110(2):506–512
- Klabunde RE, Burke SE, Henking J (1990) Enhanced lytic efficacy of multiple bolus injections of tissue plasminogen activator in dogs. *Thromb Res* 58(5):511–517
- Clark RG, Jansson JO, Isaksson O (1985) Intravenous growth hormone: growth responses to patterned infusions in hypophysectomized rats. *J Endocrinol* 104:53–61
- Belchetz PE, Plant TM, Nakai Y (1978) Hypophysial responses to continuous and intermittent delivery of hypothalamic gonadotropin-releasing hormone. *Science* 202(4368):631–633
- Vaage J, Pauly JL, Harlos JP (1987) Influence of the administration schedule on the therapeutic effect of interleukin-2. *Int J Cancer* 39(4):530–533
- Kikuchi A, Okano T (2002) Pulsatile drug release control using hydrogels. *Adv Drug Deliv Rev* 54(1):53–77
- Qui Y, Park K (2001) Environment-sensitive hydrogels for drug delivery. *Adv Drug Deliv Rev* 53(3):321–339
- Brazel CS, Peppas NA (1996) Pulsatile local delivery of thrombolytic and antithrombotic agents using poly(N-isopropylacrylamide-co-methacrylic acid) hydrogels. *J Control Release* 39(1):57–64
- Tanaka T, Fillmore D (1979) Kinetics of swelling of gels. *J Chem Phys* 70(3):1214–1218

19. Imran AB, Seki T, Takeoka Y (2010) Recent advances in hydrogels in terms of fast stimuli responsiveness and superior mechanical performance. *Polym J* 42:839–851
20. Zhang X, Wu D, Chu CC (2004) Synthesis and characterization of partially biodegradable, temperature and pH sensitive Dex–MA/PNIPAAm hydrogels. *Biomaterials* 25(19):4719–4730
21. Wu XS, Hoffman AS, Yager P (1992) Synthesis and characterization of thermally reversible macroporous poly(N-isopropylacrylamide) hydrogels. *J Polym Sci Part A Polym Chem* 30(10):2121–2129
22. Kaneko Y, Sakai K, Kikuchi A, Yoshida R, Sakurai Y, Okano T (1995) Influence of freely mobile grafted chain length on dynamic properties of comb-type grafted poly(N-isopropylacrylamide) hydrogels. *Macromolecules* 28(23):7717–7723
23. Xue W, Hamley IW, Huglin MB (2002) Rapid swelling and deswelling of thermoreversible hydrophobically modified poly(N-isopropylacrylamide) hydrogels prepared by freezing polymerization. *Polymer* 43(19):5181–5186
24. Zhang XZ, Zhuo RX (2000) Preparation of fast responsive, thermally sensitive poly(N-isopropylacrylamide) gel. *Eur Polym J* 36(10):2301–2303
25. Zhang XZ, Zhuo RX (2002) Synthesis and properties of thermosensitive poly(N-isopropylacrylamide-co-methyl methacrylate) hydrogel with rapid response. *Mater Lett* 52(1–2):5–9
26. Cheng SX, Zhang JT, Zhuo RX (2003) Macroporous poly(N-isopropylacrylamide) hydrogels with fast response rates and improved protein release properties. *J Biomed Mater Res* 67A(1):96–103
27. Zhang JT, Cheng SX, Huang SW, Zhu RX (2003) Temperature-sensitive poly(N-isopropylacrylamide) hydrogels with macroporous structure and fast response rate. *Macromol Rapid Commun* 24(7):447–451
28. Lugo-Medina E, Licea-Claverie A, Comejo-Bravo JM, Arndt KF (2007) Effect of method of preparation on properties of temperature and pH-sensitive gels: chemical crosslinking versus irradiation with e-beam. *React Funct Polym* 67(1):67–80
29. Serrano-Medina A, Comejo-Bravo JM, Licea-Claverie A (2012) Synthesis of pH and temperature sensitive, core–shell nano/microgels, by one pot, soap-free emulsion polymerization. *J Colloid Interface Sci* 369(1):82–90
30. Obeso-Vera C, Comejo-Bravo JM, Serrano-Mediana A, Licea-Claverie A (2013) Effect of crosslinkers on size and temperature sensitivity of poly(N-isopropylacrylamide) microgels. *Polym Bull* 70:653–664
31. Parr GM, Oliver WC (1992) Measurement of thin film mechanical properties using nanoindentation. *MRS Bull* 17(7):28–33
32. Fernandez VVA, Tepale N, Sanchez-Diaz JC, Mendizabal E, Puig JE, Soltero JFA (2006) Thermoresponsive nanostructured poly(N-isopropylacrylamide) hydrogels made via inverse microemulsion polymerization. *Colloid Polym Sci* 284(4):387–395
33. Fernandez VVA, Aguilar J, Becerra F, Sanchez-Diaz JC, Soltero JFA, Ortega-Gudiño P, Hernandez E, Bautista F, Puig JE (2013) Tailoring thermoresponsive nanostructured poly(N-isopropylacrylamide) hydrogels made with poly(acrylamide) nanoparticles. *Colloid Polym Sci* 291(8):1829–1842
34. Nuño-Donlucas SM, Sánchez Diaz JC, Rabelero M, Cortes-Ortega J, Luhrs-Olmos CC, Fernandez-Escamilla VVA, Mendizábal E, Puig JE (2004) Microstructured polyacrylamide hydrogels made with hydrophobic nanoparticles. *J Colloid Interface Sci* 270(1):94–98
35. Zhang XZ, Zhuo RZ (1999) A novel method to prepare a fast responsive, thermosensitive poly(N-isopropylacrylamide) hydrogel. *Macromol Rapid Commun* 20(4):229–231
36. Qin A, Lu M, Liu Q, Zhang P (2007) Synthesis and characterization of thermo-sensitive poly (N-isopropylacrylamide) hydrogel with fast response rate. *Front Chem Chin* 2(2):135–139
37. Musch J, Shneider S, Linder P, Richtering W (2008) Unperturbed volume transition of thermosensitive poly(N-isopropylacrylamide) microgel particles embedded in a hydrogel matrix. *J Phys Chem B* 112(20):6309–6314
38. Peppas N, Leobandung W (2004) Stimuli-sensitive hydrogels: ideal carriers for chronobiology and chronotherapy. *J Biomater Sci Polym Ed* 15(2):125–144